Pergamon

PII: S0042-6989(96)00319-7

Vision Res., Vol. 37, No. 13, pp. 1761–1767, 1997

Printed in Great Britain
0042-6989/97 $17.00 + 0.00

The Effects of Distractor Elements on Direction Discrimination in Random Gabor Kinematograms

PETER J. BEX,*† CURTIS L. BAKER, JR*

Received 13 July 1995; in revised form 12 August 1996

For both Fourier and non-Fourier moving patterns, models have been proposed which detect motion based on either the net orientation of energy in the stimulus (after a nonlinear stage for non-Fourier motion stimuli) or on the changes in the relative locations of spatial primitives in the image. Both approaches have been successful in accounting for detection of simple translational displacements, but we examined how such models coped with more demanding stimuli. We examined direction discrimination using two-flash random Gabor kinematograms which selectively reveal Fourier and non-Fourier motion mechanisms. In addition to target elements, multiple distractor elements were added, either static or randomly moving. It was found that detection of Fourier motion was relatively unaffected by the distractors unless they were of orthogonal orientation. Detection of non-Fourier motion was possible, but with a slightly higher error rate, even with many distractors and was not at all affected by orthogonal distractors. The results for distractors of the same orientation as targets are in better agreement with predictions of energy than with edge-matching models. The differing effects of orthogonal distractors further strengthen the proposed dichotomy of quasi-linear and nonlinear motion mechanisms, but indicate that the latter operates on a more complex representation than a simple contrast envelope. © 1997 Elsevier Science Ltd.

Motion Linear Nonlinear Non-Fourier Feature-tracking

INTRODUCTION

Since the early experiments of Anstis (1970) and Braddick (1974), random dot kinematograms (RDKs) have become widespread stimuli in human motion psychophysics. Their popularity is based on the observation that under appropriate conditions, motion may be seen between spatially displaced, correlated regions of random dot fields when they are presented successively. Motion may be seen even though the correlated regions are not readily distinguishable when each flash is inspected separately, precluding the idea that objects are detected whose change of position is later perceived as motion. Braddick's original suggestion was that this phenomenon revealed a hard-wired, "short-range" motion mechanism distinct from higher level "long range" object-tracking processes. The short-range process was originally thought to detect small spatial displacements within a short time-scale (Braddick, 1974; Anstis, 1980; Baker & Braddick, 1985). Subsequently, many studies have investigated the effects on direction discrimination of manipulations of the spatial structure of RDKs. There have been a number of studies which have examined the effects of band-pass and low-pass spatial frequency filtering on d_{max}, the maximum displacement which supports motion perception. Despite design differences, the general finding in these studies is that d_{max} is inversely related to spatial frequency for band-pass filtered RDKs (Chang & Julesz, 1983, 1985; Bischof & Di Lollo, 1990; Cleary & Braddick, 1990a; Cleary, 1990). For low-pass filtered RDKs, the effect of filtering on d_{max} is more complicated. Here the general finding is that when the upper cut-off of the low-pass filter is relatively high, there is little or no effect of low-pass filtering on d_{max}. However, when the upper cut-off is below a critical spatial frequency, d_{max} scales inversely with the cut-off of the low-pass filter (Cleary & Braddick, 1990b; Bischof & Di Lollo, 1990; Morgan & Mather, 1994).

Two general classes of model have been proposed to account for these results. The first of these argues that motion is detected by a range of mechanisms each narrowly tuned for spatial and temporal frequency (e.g. Adelson & Bergen, 1985; van Santen & Sperling, 1985; Watson & Ahumada, 1985; for review, see Nakayama, 1985). Despite computational differences among these models, the perceived direction of a moving image corresponds to the net orientation of the spatio-temporal Fourier power spectrum (motion energy) and is based upon analysis across multiple spatial and temporal scales.

*McGill Vision Research Unit, Department of Ophthalmology, McGill University, 687 Pine Avenue West, Montreal, Canada H3A 1A1.
†To whom all correspondence should be addressed at present address: Center for Visual Science, 274, Meliora Hall, Rochester, New York 14627-0268, U.S.A. [*Email*: bex@cvs.rochester.edu].

The direction signals across spatial scales are later combined to indicate the overall direction of movement. The rules for the combination of directional signals across spatial scales remain to be defined and this issue is discussed elsewhere (Cleary & Braddick, 1990b; Brady *et al.*, 1997).

Alternative models of motion detection involve analysis at a single scale. Morgan (1992), Morgan & Fahle (1992), Morgan & Mather (1994) and Eagle & Rogers (1996) have argued that the identification of spatial primitives precedes motion detection. In these models, spatial primitives are determined by zero crossings (Marr & Hildreth, 1980), zero bounded regions (ZBRs) according to one or other variant of the MIRAGE model (Watt & Morgan, 1983), or at the local peaks in the luminance distribution of a pattern (Eagle & Rogers, 1996). Once the location of the spatial primitives in a RDK has been determined, the direction of motion is calculated from nearest-neighbor correspondences between like-signed spatial primitives in each frame. Thus, $d_{\max}$ will equal approximately half the mean separation between like-signed spatial primitives.

For simple translational motion of broad-band and narrow-band images, both single scale and multi-scale models have been shown to be successful in accounting for motion detection for spatially filtered RDKs (see, for example, Eagle & Rogers, 1996). However, we examined how such models performed when confronted with more demanding stimuli. We employed random Gabor kinematogram stimuli which allow independent control of element density and stimulus band-width. Previous studies have shown that $d_{\max}$ in these patterns varies with element density (Boulton & Baker, 1993a,b). At high micropattern densities, $d_{\max}$ is dependent on the spatial frequency of the carrier sine grating, consistent with either class of motion detection model. At low element densities, $d_{\max}$ is dependent on the envelope frequency, which is proportional to the inter-element separation (Boulton & Baker, 1993a,b).

In addition to target Gabor micropatterns which were coherently shifted between flashes, distracting micropatterns were added to each flash of the random Gabor kinematogram. The distractors were identical in spatial structure to the target micropatterns (Gabors) but they were not coherently displaced between flashes. We investigated the effects on direction discrimination of distractors of equal and orthogonal orientation to targets and compared the performance of observers to that of motion energy and edge-matching models.

METHODS

Stimuli were generated using a VSG 2/1 graphics card (Cambridge Research Systems) in a host PC microcomputer (DELL 333D). Stimuli were presented on a Nanao Flexscan 6500 monitor with P4 phosphor and with a frame rate of 118 Hz. The image was 16 deg horizontally (512 pixels) by 13.4 deg vertically (428 pixels) and was viewed from a distance of 118 cm. The mean luminance of the display was 32 cd/m^2. The luminance of the display was carefully linearized using an ISR attenuator (Pelli & Zhang, 1991) and linearity was calibrated using a UDT Photometer.

Stimuli

The stimuli were arrays of Gabor micropatterns distributed pseudo-randomly across the display field. Each Gabor was a one-dimensional sine grating multiplied by a two-dimensional Gaussian window:

$$L_{(x,y)} = L_0\left\{1 + C_{\exp}[-x^2/2\sigma_x^2 - y^2/2\sigma_y^2 * \sin(2\pi x/\lambda + \phi)\right\} \quad (1)$$

where L_0 = mean luminance; C = contrast; σ_x = horizontal Gaussian width parameter; σ_y = vertical Gaussian width parameter; λ = wavelength; ϕ = phase of the sine wave.

In the present experiments, the spatial frequency of the sine-wave carrier was 2 c/deg ($\lambda = 16$ pixels) and $\sigma_x = \sigma_y = 0.75\lambda$. The carrier was in sine phase (phase = 0 deg at center) to ensure that the Gabor was DC balanced. The peak contrast of the Gabors was 25% in all conditions. The micropatterns were placed along two strips across the top and bottom of the stimulus field (approximately 2 deg above and below the fixation point) to confine the stimulus in eccentricity and to prevent the observers from paying attention to a fortuitous stimulus "feature" (e.g. a relatively isolated micropattern) close to the fixation point. On each trial the micropatterns were placed on a notional grid and were spaced equally across each row. The location of each micropattern on each row was randomly jittered horizontally and vertically by ± 1.2 deg and the whole row was then jittered horizontally by $\pm$ half the mean inter-pattern separation. There was wrap-around applied at the display boundaries. These manipulations of spatial position using random jitter ensured that the micropatterns were evenly distributed across the visual field whilst periodicity and clustering were avoided both horizontally and vertically.

Following Boulton & Baker (1993a,b), two viewing conditions were employed, termed quasi-linear and nonlinear. Under quasi-linear viewing conditions, $d_{\max}$ was found to correspond to approximately half a cycle of the carrier frequency of the target Gabors. Quasi-linear motion was optimal at high densities and short exposure durations. Therefore, for quasi-linear conditions we used an exposure duration and stimulus onset asynchrony (SOA) of 80 msec (there was no ISI—interstimulus interval) and the target density was high (16 micropatterns per row, 64 target micropatterns per flash). These authors identified nonlinear motion when the SOA was long and when target density was low. Therefore, for nonlinear conditions we also used an exposure duration of 80 msec but with a 120 msec SOA (there was a 40 msec ISI). During the ISI, the screen was a blank field of mean luminance. We used a low target density (three micropatterns per row, 12 target micropatterns per flash). At this target density, motion detection behavior was consistently nonlinear, whilst several distractor micropatterns could be added before the density became too

high for the postulated nonlinear mechanism to work. A range of ISIs and densities were tested experimentally and it was found that direction discrimination was qualitatively similar for a range of conditions similar to those we selected. In addition to the target micropatterns, distractor micropatterns were added to each flash. The number of micropatterns was either 0 or twice the number of targets (i.e., 32 per row for quasi-linear conditions, 6 per row for nonlinear conditions). In one condition (static) the distractors were presented in the same location on each flash, in another condition (dynamic) the distractors were randomly repositioned between flashes.

Psychophysical procedure

Subjects were seated at the required viewing distance and were instructed to fixate a small spot in the center of the screen. The screen was blank and at the mean luminance. Subjects pressed a response key to initiate each trial. There followed a two-flash apparent motion sequence. Subjects were required to indicate by pressing a response key, in which direction the micropatterns had moved, left or right. There was no feedback. A range of displacements was set according to a method of constant stimuli to cover the range at which there were fewest errors to displacements at which there were most errors. There were five levels, each was presented ten times in random order on each run and there were four runs for each condition. This procedure was repeated a minimum of four times for each condition, the mean of which is reported.

Model simulations

Responses of two kinds of models were simulated for comparison to the psychophysical data, using custom functions written in MatLab (Mathworks, Inc.) software. The execution times were tractable only in the case of spatially one-dimensional models—such model results are entirely reasonable to compare to experiments in which the motion is orthogonal to the orientation of the stimuli (in this case, for vertical distractors); it was not feasible to attempt modeling of experiments involving horizontal distractors. Stimuli were represented as conventional space–time arrays, with spatial position along a profile taken through one row of micropatterns in an actual stimulus. The simulated stimuli were programmed to mimic the actual stimuli as closely as possible, using the same gridding and jittering methods.

Each model operated on such a space–time array, and produced a scalar signal of strength of motion, which was linked to a "right" vs "left" decision according to its sign, and logged as a correct or erroneous trial according to whether this agreed with the actual direction of simulated motion. Because of the positional jittering, which was independently random on each trial, it was necessary to simulate many repetitions of the same stimulus conditions. The simulation looped through 60 sets of five displacements, and tallied the accumulated percentage errors as a function of displacement, as in psychophysical experiments. This was repeated for various numbers of distractors, for two sets of conditions, quasi-linear (high density/short SOA) and nonlinear (low density/long SOA).

An Adelson–Bergen model was implemented as a set of space–time oriented linear filters [as in Fig. 9(a) of Adelson & Bergen, 1985], which were functions of spatial offset, s, and time lag, t:

$$h(s, t) = e(-s^2/2\sigma_s^2 - t^2/2\sigma_t^2)\sin(2\pi s/\lambda_s + 2\pi kt/\lambda_t + \phi) \quad (2)$$

where λ_s = spatial wavelength, λ_t = temporal period, $\sigma_s = \lambda_s/2$, $\sigma_t = \lambda_t/2$, ϕ = phase, and $k = +1$ or -1 to specify direction. (Note that λ_s and λ_t are reciprocals of the filter's optimal spatial and temporal frequency, respectively.) λ_s and λ_t were set to values determined to be optimal for detection of motion of the stimuli (see below).

Directional responses were taken from the net sum of squares of responses of convolution responses of sine ($\phi = 0$) and cosine ($\phi = 90$) pairs of these filters. To simulate a second-order, nonlinear energy model, the space–time array was first full-wave rectified before convolution with the space–time filters (Chubb & Sperling, 1988). The only parameters of this model were those of the spatio-temporal filter function. Its optimal spatial and temporal wavelengths were specified from the peak position of the spatio-temporal frequency power spectrum of a representative space–time stimulus array. For a stimulus with high density and short SOA, the optimal spatial wavelength was simply that of the stimulus micropatterns; the optimal temporal period was 366 msec. For a low density stimulus with longer SOA, the optimal spatial wavelength was 170 pixels (5.3 deg) and the temporal period was 512 msec. The spatial and temporal bandwidths were both specified by setting $\sigma = \lambda/2$.

An edge-matching model was implemented by extracting two spatial profiles from the stimulus space–time array, one for each flash; zero-crossing tokens were extracted from each of these profiles by searching for instances of the profile having successive points, one below a threshold level ($-\theta$) and an adjacent one above $+\theta$. For each such token in the first profile, the nearest like-signed neighbors to the left and right of it in the second profile were determined, and the nearer of the two was taken as the correspondence match. This match contributed +1 or −1 to a tally, according to whether it corresponded to left or right displacement. The sign of this tally determined a left or right decision for a given trial. The only parameter in this model was the threshold, θ, specified as a percentage of the amplitude of a single stimulus micropattern. Pilot simulations showed this parameter must be small enough (less than about 0.05) to generate at least three tokens for an isolated Gabor micropattern, to avoid grossly pathological behavior; subject to this constraint, simulation results showed surprisingly minor sensitivity to changes in the threshold value. Early results showed the greatest performance problems for this model was in the case of low density/

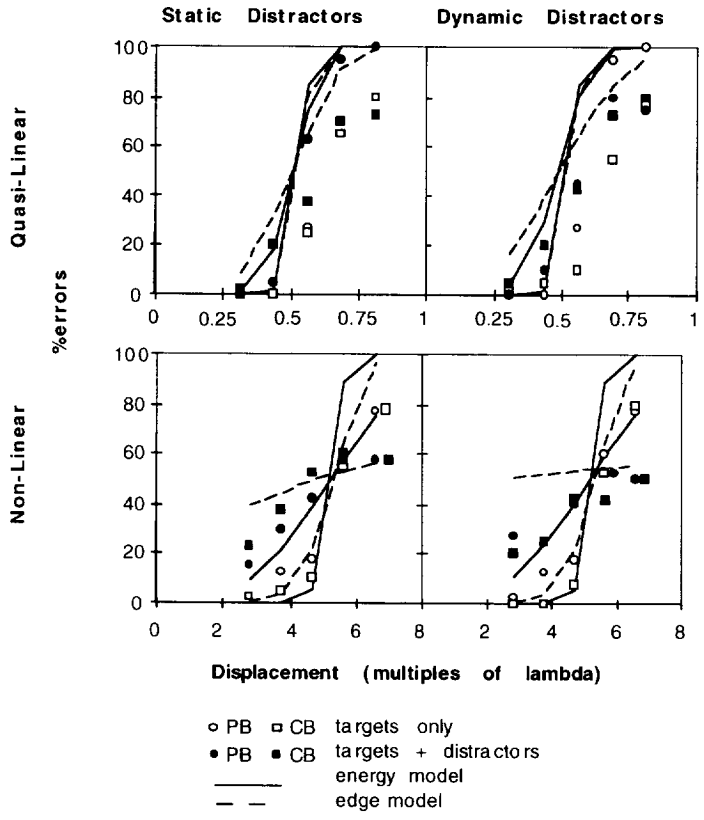

FIGURE 1. The effects of vertical distractor elements on direction discrimination in random Gabor kinematograms. Errors in direction discrimination are shown for two observers (circular and square symbols) as a function of displacement size (plotted as multiples of the carrier wavelength, 0.5 deg). Open symbols show errors when no distractors were present, closed symbols show errors when the number of distractors was equal to twice the number of targets. For clarity, overlapped data points have been shifted slightly to the right. The upper row shows data for viewing conditions which isolate a quasi-linear motion mechanism: high target density (64 targets per flash) and short stimulus onset asynchrony (80 msec). The lower row shows data for viewing conditions which isolate a nonlinear motion mechanism: low target density (12 targets per flash) and long SOA (120 msec). The left column shows data for static distractors (i.e., distractors in the same position for each flash), the right column shows data for dynamic distractors (i.e., distractors were randomly repositioned on each flash). Solid lines show the psychometric functions of a motion energy model (after full-wave rectification for nonlinear viewing conditions), broken lines show the psychometric function of an edge-matching model. In all cases the steeper model slopes were recorded when no distractors were present. A higher error rate in the presence of distractors resulted in shallower functions for both observers and models.

long SOA, so we ran a large number of simulations for such a case to empirically determine the value of this parameter (0.002) to give the edge-matching model its best performance.

RESULTS

In the absence of any distractors, direction discrimination performance for quasi-linear viewing conditions (high density/short SOA) was perfect for a range of small displacements, then rose very rapidly to worse than chance (i.e., perceived motion was opposite to the veridical), as shown by the open symbols (squares and circles for the two observers) in the top panels of Fig. 1. The chance performance at displacements close to one-half of the carrier spatial cycle, λ, and reversal of perceived direction for larger displacements, are diagnostic of a quasi-linear motion mechanism which is closely related to the structure of the micropattern carrier (Boulton & Baker, 1993a). The closed symbols in the top row of Fig. 1 show the results when distractors were added; both static (upper left panel) and dynamic vertical distractors (upper right panel) caused almost no disruption of performance for quasi-linear conditions.

For nonlinear viewing conditions (low density, long SOA), in the absence of distractors (Fig. 1, open symbols in lower panels), direction discrimination was possible at much larger displacements than for quasi-linear viewing conditions. Chance performance is reached at displacements of about five times the carrier wavelength; i.e., d_{max} was determined by the envelope, not the internal carrier structure of the micropatterns (Boulton & Baker, 1993a,b). Vertical distractors produced a moderate increase in direction discrimination errors at small displacements that was approximately equal for both static and dynamic distractors (filled symbols in lower panels of Fig. 1).

Since the ratio of distractors to targets was kept the same (2:1), the data of Fig. 1 show a greater effect of distractors on nonlinear motion, than on quasi-linear motion—this in itself should not be too surprising, since a nonlinearity discards information—nevertheless, the performance was still quite good (and even better for lower ratios of distractors to targets, in data not shown

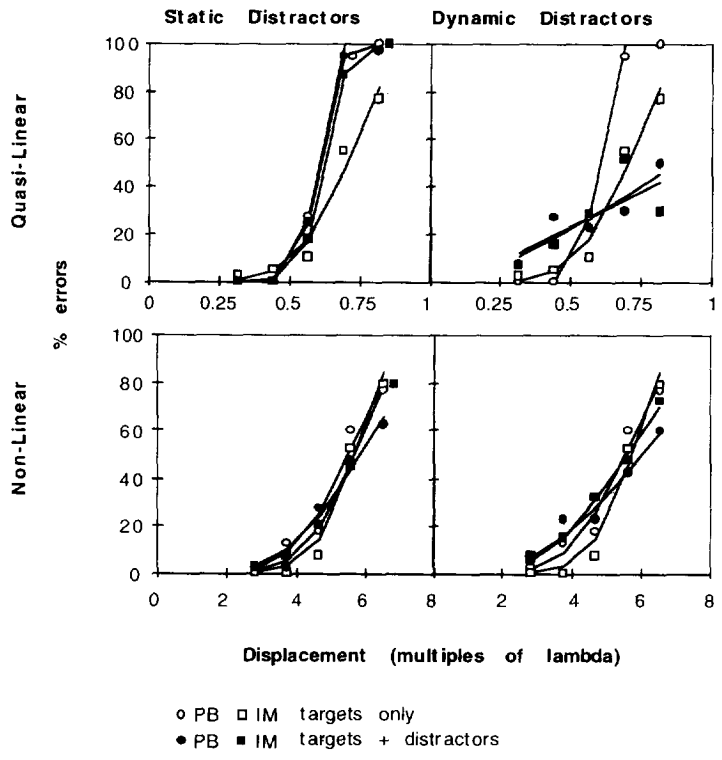

FIGURE 2. The effects of horizontal distractors elements on direction discrimination in random Gabor kinematograms. The data are plotted in the same way as for Fig. 1, except that the distractors were Gabor micropatterns whose carriers were horizontally oriented (orthogonal to the targets). The solid lines are Weibull curve-fits to the data.

here). We compared this performance with that of two models of motion detection, described above, using exactly the same stimulus conditions. The lines in Fig. 1 show Weibull curve-fits (Weibull, 1951) to the psychometric functions produced by the two models—the solid lines in each case show the performance of the motion energy model (after full-wave rectification for nonlinear conditions), and the broken lines show the performance of the edge-matching model. Each plot shows two sets of each kind of line; in all cases, lines which are closer to chance performance are those representing model performance in the presence of distractors, while the lines further from chance show results for targets only. Both models showed similarly good performance for all the quasi-linear conditions and were similar to the psychophysical data (except for under-prediction of d_{max}—see below).

For nonlinear conditions in the absence of distractors, both models showed similar performance, and both were consistent with the observers' psychophysical data (Fig. 1, lower panels). However, when vertical distractors were added, the edge-matching model collapsed to near chance performance (upper set of dashed lines in lower panels of Fig. 1). The motion energy model (preceded by a full-wave rectifying nonlinearity) was resistant to the noise of distractors for nonlinear conditions (solid lines in lower panels of Fig. 1), predicting better than chance performance like that of the observers.

Figure 2 shows the data for horizontal distractors (carrier orthogonal to that of the targets), plotted in a similar manner to Fig. 1, except that the lines indicate Weibull curve-fits to the measured psychophysical data. (As stated earlier, it was not feasible to simulate models with horizontal distractors.) The upper panels in Fig. 2 show results for quasi-linear viewing conditions. Again, the psychometric functions tend to pivot about a chance performance for displacements of slightly more than half a cycle of the carrier. Static distractors (upper left panel) had no systematic effect, but dynamic horizontal distractors (upper right panel) produced a very different pattern of results: the shape of the psychometric function became much shallower, and the reversal in apparent direction was lost. This pattern is quite different from that for vertical distractors (Fig. 1, upper panels), in which dynamic and static distractors alike had negligible effect on performance.

Even more surprising were the effects of orthogonal distractors under nonlinear viewing conditions (Fig. 2, lower panels); in marked contrast to the results for vertical distractors (Fig. 1, lower panels), orthogonal distractors had a negligible effect on direction discrimination. This immunity to orthogonal distractors was found regardless of whether they were static or dynamic.

DISCUSSION

Under quasi-linear viewing conditions (high target density, short SOA), direction discrimination was relatively unaffected by the presence of distracting micropatterns which had the same spatial structure, but were not coherently displaced with target micropatterns. Direction discrimination was affected under

these conditions only when the distractors were dynamic and were oriented orthogonal to the axis of motion of the targets. For nonlinear viewing conditions (low target density, long SOA), direction discrimination was affected by distractors only if they were of the same orientation.

The effect of distractors on quasi-linear viewing conditions

For motion energy detection, the direction of movement is indicated by the net orientation of motion energy in the stimulus and this was relatively unaffected by the addition of distractor micropatterns. Consequently, the energy-based model was relatively unaffected by the distractor micropatterns. For the edge-matching model, direction discrimination was limited by the correspondences between the edges in the first and second flashes of the image. Nearest-neighbor edge-matching was also resistant to false correspondences among the spatial primitives in distractor and target micropatterns because of the local nature of the matching process. Both models performed very similarly in comparison to the psychophysical data for quasi-linear viewing conditions.

For quasi-linear conditions with no distractors, the estimates of d_{max} (81% correct performance, in Weibull curve-fits) were as follows expressed as fractions of the carrier wavelength (0.5 deg): PB = 0.63; CB = 0.74; motion energy = 0.55; edge-matching = 0.55. Both models produced values of d_{max} somewhat lower than the human results. For motion energy models, this may be accounted for by a contribution of a weak motion signal in the correct direction at spatial frequencies lower than λ in the Gabor stimulus. The model used here only simulated a single set of filters, those tuned to the peak spatial frequency of the stimuli; a fuller implementation of such a model, incorporating multiple energy model filters tuned to a series of spatial scales, could in principle account for a larger d_{max}. This would require the application of additional weighting to motion signals at low spatial frequencies. Edge-based models, at least as presently formulated (e.g., Morgan, 1992), are inherently single-channel in nature; it is unclear how models of this sort could be modified to account for the higher d_{max} value achieved by observers, other than by an implementation which operates separately on each of a series of spatial scales.

When the distractors were horizontal (orthogonal to the targets) and dynamic, it might be expected that this should produce little or no effect on the perceived motion of the targets because of the narrow orientation tuning of motion energy detectors (e.g. Adelson & Bergen, 1985). An edge-based model would also be specific to edge orientation, and thus also to show little effect of orthogonal distractors. (Note, however, that a model like that used by Eagle & Rogers, 1996 which matches local, non-oriented peaks, would behave differently.) The data showed that although direction discrimination was relatively unaffected for small displacements, dynamic, horizontal distractors eliminated the reversals in the psychometric function (Fig. 2, top panels). There are a variety of reasons why the reversal regions of performance might be more fragile and vulnerable to added noise, but it is notable that the vulnerability was so much greater for orthogonal than for like-orientation distractors. Observers also reported that direction discrimination was far more difficult with dynamic orthogonal distractors, whereas the random motion of the dynamic vertical distractors was "captured" by the coherent motion of the targets (see Ramachandran & Cavanagh, 1987). Snowden (1989) has shown that in random dot kinematograms, direction discrimination was impaired by the presence of additional dots moving in an orthogonal direction to that of the target dots. Snowden argued that competitive interactions between directionally sensitive channels resulted in suppression between motion in orthogonal directions. The present data are consistent with this proposal, for quasi-linear but not for nonlinear viewing conditions.

The effect of distractors on nonlinear viewing conditions

Under nonlinear viewing conditions, the substantial increase in displacement limits has been attributed to a nonlinear motion detection mechanism (Boulton & Baker, 1993a,b). The present results are in good agreement with their data and support their proposal that different mechanisms mediate motion detection at different densities and SOAs. It has been suggested (Smith, 1994; Bex & Baker, 1995) that in principle, nonlinear motion detection could involve either high-level feature-tracking mechanisms, which track the change in position over time of features (Ullman, 1979), or low-level energy-based mechanisms which receive rectified inputs (Chubb & Sperling, 1988; Wilson *et al.*, 1992; Werkhoven *et al.*, 1993).

As discussed above for quasi-linear viewing conditions, motion energy mechanisms are less affected by distractors because the net orientation of motion energy is relatively unaffected by the distractors (after nonlinear rectification in the present case). The nonlinear motion energy model, therefore, showed an increase in error rate at small displacements, but performed at well above chance levels. The nearest neighbor edge-matching model was vulnerable to false correspondences over larger spatial displacements and direction discrimination was effectively at chance in the presence of distractors. The noise-rejection properties of such models (e.g., see Watt & Morgan, 1983) are effective against low-amplitude, broad-band noise, but would not be for the noise used here—the distractors were of the same contrast and band-width as the targets, so their zero-bounded regions would have too large a "mass" to be discounted. The psychophysical data for vertical distractors were more consistent with the nonlinear motion energy model than with nearest-neighbor edge-matching.

When the distractors were horizontal, whether dynamic or static, their presence had very little effect on direction discrimination for nonlinear viewing conditions (Fig. 2, lower panels). However, with no distractors present, it has been shown that direction discrimination is

possible between Gabors of orthogonal orientation (Boulton & Baker, 1994) for nonlinear (but not for linear) viewing conditions. It therefore seemed quite surprising that orthogonal distractors did not disrupt motion detection. This behavior was in marked contrast to the disruptive effects of horizontal distractors in our data for quasi-linear conditions (Fig. 2, lower panels) and in the data of Snowden (1989). These observations suggest that the nonlinear motion mechanism might be somewhat more complicated than a simple full-wave rectification prior to a motion energy model.

With no distractors, the present data and those of Boulton & Baker (1993a) show that at high target densities, d_{max} was relatively small (equal to the half cycle limit of the carrier sine grating). The present data show that at high micropattern densities, it is possible to create conditions where direction discrimination can be accurate at displacements much larger than those predicted from the carrier sine grating. This may be achieved using a low target density but a high total density because of the presence of distractors. For a given micropattern density, it seems paradoxical that d_{max} may be increased by reducing the number of coherently moving targets and thereby reducing the signal: noise ratio. This suggests that density *per se* is not a critical factor precluding the operation of nonlinear motion mechanisms, but that it is the density of *coherently* moving target patterns that is important.

REFERENCES

Adelson, E. H. & Bergen, J. R. (1985). Spatio-temporal energy models for the perception of motion. *Journal of the Optical Society of America A, 2*, 284–299.

Anstis, S. M. (1970). Phi movement as a subtractive process. *Vision Research, 10*, 1411–1430.

Anstis, S. M. (1980). The perception of apparent movement. *Philosophical Transactions of the Royal Society of London B, 290*, 153–168.

Baker, C. L. & Braddick, O. J. (1985). Eccentricity-dependent scaling of the limits for short-range apparent motion perception. *Vision Research, 25*, 803–812.

Bex, P. J. & Baker, C. L. (1995). Effects of band-limited noise on quasi-linear and nonlinear mechanisms of motion detection. *Investigative Ophthalmology and Visual Science, 36*, (Suppl. 635).

Bischof, W. F. & Di Lollo, V. (1990). Perception of directional sampled motion in relation to displacement and spatial frequency: evidence for a unitary motion system. *Vision Research, 30*, 1341–1362.

Boulton, J. C. & Baker, C. L. (1993a) Different parameters control motion perception above and below a critical density. *Vision Research, 33*, 1803–1811.

Boulton, J. C. & Baker, C. L. (1993b) Dependence on stimulus onset asynchrony in apparent motion: evidence for two mechanisms. *Vision Research, 33*, 2013–2019.

Boulton, J. C. & Baker, C. L. (1994). Psychophysical evidence for both a "quasi-linear" and a "nonlinear" mechanism for the detection of motion. In Lawton, T. B. (Ed.), *Computational vision based on neurobiology*, S.P.I.E. Proc. 2054, pp. 124–133.

Braddick, O. J. (1974). A short-range process in apparent motion. *Vision Research, 14*, 519–527.

Brady, N., Bex, P. J. & Fredericksen, R. E. (1997). Independent coding across spatial scales in moving fractal images. *Vision Research, 37*, 1873–1883.

Chang, J. J. & Julesz, B. (1983). Displacement limits for spatial frequency filtered random dot cinematograms in apparent motion. *Vision Research, 23*, 1379–1385.

Chang, J. J. & Julesz, B. (1985). Cooperative and non-cooperative processes of apparent movement of random-dot cinematograms. *Spatial Vision, 1*, 39–45.

Chubb, C. & Sperling, G. (1988). Drift-balanced random stimuli: a general basis for studying non-Fourier motion perception. *Journal of the Optical Society of America A, 5*, 1986–2007.

Cleary, R. (1990). Contrast dependence of short-range apparent motion. *Vision Research, 30*, 463–478.

Cleary, R. & Braddick, O. J. (1990a) Direction discrimination for band-pass filtered random dot kinematograms. *Vision Research, 23*, 303–316.

Cleary, R. & Braddick, O. J. (1990b) Masking of low frequency information in short-range apparent motion. *Vision Research, 30*, 317–327.

Eagle, R. A. & Rogers, B. J. (1996). Motion detection is limited by element density not spatial frequency. *Vison Research, 36*, 545–558.

Marr, D. & Hildreth, E. (1980). Theory of edge detection. *Proceedings of the Royal Society of London B, 207*, 187–217.

Morgan, M. J. (1992). Spatial filtering precedes motion detection. *Nature, 355*, 344–346.

Morgan, M.J. & Fahle, M. (1992). Effects of pattern element density upon displacement limits for motion detection in random binary luminance patterns. *Proceedings of the Royal Society of London B, 248*, 189–198.

Morgan, M. J. & Mather, G. (1994). Motion discrimination in two-frame sequences with differing spatial frequency content. *Vision Research, 34*, 197–208.

Nakayama, K. (1985). Biological image motion processing: a review. *Vision Research, 25*, 625–660.

Nishida, S. & Sato, T. (1995). Motion aftereffect with flickering test patterns reveals higher stages of motion processing. *Vision Research, 35*, 477–490.

Pelli, D. & Zhang, L. (1991). Accurate control of contrast on microcomputer displays. *Vision Research, 31*, 1337–1350.

Ramachandran, V. S. & Cavanagh, P. (1987). Motion capture anisotropy. *Vision Research, 27*, 97–106.

Smith, A. T. (1994). Correspondence-based and energy-based detection of second-order motion in human vision. *Journal of the Optical Society of America A, 11*, 1940–1948.

Snowden, R. J. (1989). Motions in orthogonal directions are mutually suppressive. *Journal of the Optical Society of America A, 6*, 1096–1101.

Ullman, S. (1979). *The interpretation of visual motion*. Cambridge, MA: MIT Press.

van Santen, H. & Sperling, G. (1985). Elaborated Reichardt detectors. *Journal of the Optical Society of America A, 2*, 300-321.

Watson, A. B. & Ahumada, A. J. (1985). Model of human visual-motion sensing. *Journal of the Optical Society of America A, 2*, 322–341.

Watt, R. J. & Morgan, M. (1983). The recognition and representation of edge blur: evidence for spatial primitives in vision. *Vision Research, 23*, 1465–1477.

Weibull, W. (1951). A statistical distribution function of wide applicability. *Journal of Applied Mechanics, 18*, 292–297.

Werkhoven, P., Sperling, G. & Chubb, C. (1993). The dimensionality of texture-defined motion: a single channel theory. *Vision Research, 33*, 463–485.

Wilson, H. R., Ferrera, V. P. & Yo, C. (1992). A psychophysically motivated model for two-dimensional motion perception. *Visual Neuroscience, 9*, 79–97.

Acknowledgements—This research was supported by Canadian NSERC grant OGPOOO1978 to Curtis Baker. We would like to thank Isabelle Mareschal for observing, Ken Charles for programming assistance, and Hugh Wilson for helpful advice on modeling.